Axion-like-particle dark matter beyond the standard paradigm

Cem Eröncel, Istanbul Technical University & MEF University

2nd General Meeting of COST Action COSMIC WISPers (CA21106), 5 September 2024

CE, R. Sato, G. Servant, P.Sørensen, *JCAP* **10** (2022) 053 [2206.14269]
CE, Servant, *JCAP* **01** (2023) 009 [2207.10111]
A. Chatrchyan, **CE**, M. Koschnitzke, G. Servant, *JCAP* **10** (2023) [2305.03756],
CE, R. Sato, G. Servant, P.Sørensen [2408.08355]

ALP dark matter: The standard paradigm

The cosmology of an ALP field ϕ is determined by the evolution equation:

$$\ddot{\phi} + 3H\dot{\phi} - \frac{\nabla^2}{a^2}\phi + V'(\phi) = 0, \quad V(\phi, T) = m_\phi^2(T) f_\phi^2 \left[1 - \cos\left(\frac{\phi}{f_\phi}\right)\right].$$

One also needs to specify the initial conditions (ICs) that depends on the time of the symmetry breaking that has generated the ALP as the pNGB.

- **Post-inflationary:** Different ICs in each Hubble patch. Inhomogeneous. $\Longrightarrow$ Mini-clusters
- **Pre-inflationary:** Random initial angle $\theta \equiv \phi/f_\phi \in [-\pi, \pi)$ in observable universe. Homogeneous.

Assuming pre-inflationary scenario and negligible initial kinetic energy

$$\begin{cases} \phi \approx \text{constant}, & m(T) \ll H(T) \\ n_\phi = \rho_\phi / m_\phi \propto a^{-3}, & m(T) \gg H(T) \end{cases}.$$

The relic density for ALP dark matter is determined by $0 \leq |\theta_i| < \pi$.

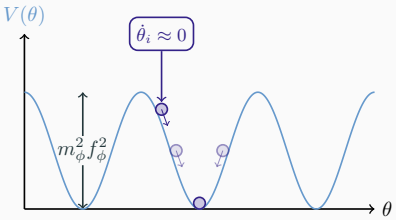

ALP dark matter: The standard paradigm

The cosmology of an ALP field ϕ is determined by the evolution equation:

$$\ddot{\phi} + 3H\dot{\phi} - \frac{\nabla^2}{a^2}\phi + V'(\phi) = 0, \quad V(\phi, T) = m_\phi^2(T) f_\phi^2 \left[1 - \cos\left(\frac{\phi}{f_\phi}\right)\right].$$

One also needs to specify the initial conditions (ICs) that depends on the time of the symmetry breaking that has generated the ALP as the pNGB.

- **Post-inflationary:** Different ICs in each Hubble patch. Inhomogeneous. $\Longrightarrow$ Mini-clusters
- **Pre-inflationary:** Random initial angle $\theta \equiv \phi/f_\phi \in [-\pi, \pi)$ in observable universe. Homogeneous.

Assuming pre-inflationary scenario and negligible initial kinetic energy

$$\begin{cases} \phi \approx \text{constant}, & m(T) \ll H(T) \\ n_\phi = \rho_\phi / m_\phi \propto a^{-3}, & m(T) \gg H(T) \end{cases}.$$

The relic density for ALP dark matter is determined by $0 \leq |\theta_i| < \pi$.

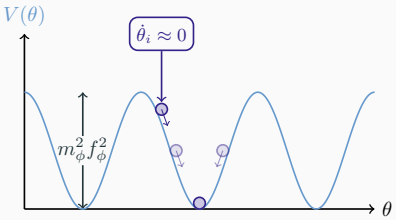

ALP dark matter: The standard paradigm

The cosmology of an ALP field ϕ is determined by the evolution equation:

$$\ddot{\phi} + 3H\dot{\phi} - \frac{\nabla^2}{a^2}\phi + V'(\phi) = 0, \quad V(\phi, T) = m_\phi^2(T) f_\phi^2 \left[1 - \cos\left(\frac{\phi}{f_\phi}\right)\right].$$

One also needs to specify the initial conditions (ICs) that depends on the time of the symmetry breaking that has generated the ALP as the pNGB.

- **Post-inflationary:** Different ICs in each Hubble patch. Inhomogeneous. $\Longrightarrow$ Mini-clusters
- **Pre-inflationary:** Random initial angle $\theta \equiv \phi/f_\phi \in [-\pi, \pi)$ in observable universe. Homogeneous.

Assuming pre-inflationary scenario and negligible initial kinetic energy

$$\begin{cases} \phi \approx \text{constant}, & m(T) \ll H(T) \\ n_\phi = \rho_\phi / m_\phi \propto a^{-3}, & m(T) \gg H(T) \end{cases}.$$

The relic density for ALP dark matter is determined by $0 \leq |\theta_i| < \pi$.

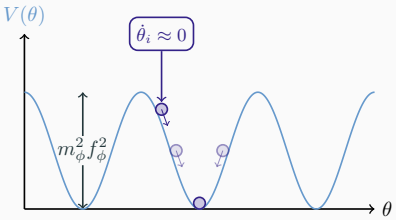

ALP dark matter: The standard paradigm

The cosmology of an ALP field ϕ is determined by the evolution equation:

$$\ddot{\phi} + 3H\dot{\phi} - \frac{\nabla^2}{a^2}\phi + V'(\phi) = 0, \quad V(\phi, T) = m_\phi^2(T) f_\phi^2 \left[1 - \cos\left(\frac{\phi}{f_\phi}\right)\right].$$

One also needs to specify the initial conditions (ICs) that depends on the time of the symmetry breaking that has generated the ALP as the pNGB.

- **Post-inflationary:** Different ICs in each Hubble patch. Inhomogeneous. $\Longrightarrow$ Mini-clusters
- **Pre-inflationary:** Random initial angle $\theta \equiv \phi/f_\phi \in [-\pi, \pi)$ in observable universe. Homogeneous.

Assuming pre-inflationary scenario and negligible initial kinetic energy

$$\begin{cases} \phi \approx \text{constant}, & m(T) \ll H(T) \\ n_\phi = \rho_\phi / m_\phi \propto a^{-3}, & m(T) \gg H(T) \end{cases}.$$

The relic density for ALP dark matter is determined by $0 \leq |\theta_i| < \pi$.

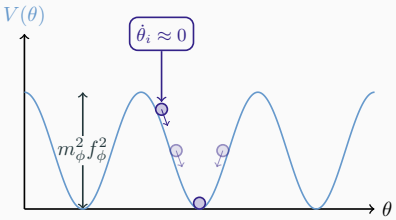

ALP dark matter parameter space in the standard paradigm (with $g_{\theta\gamma} = (\alpha_{\rm em}/2\pi)(1.92/f_\phi)$)

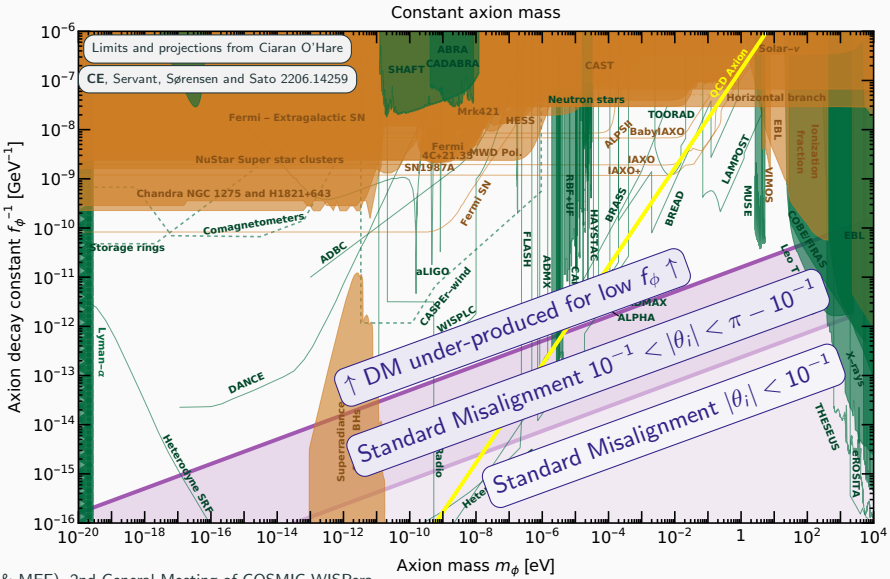

ALP dark matter parameter space in the standard paradigm (with $g_{\theta\gamma} = (\alpha_{\rm em}/2\pi)(1.92/f_\phi)$)

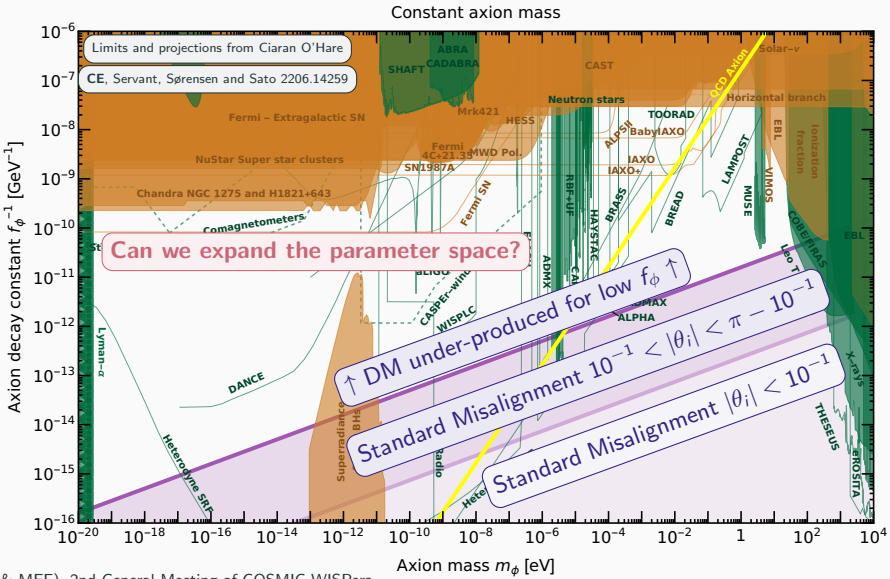

Extending the parameter space to lower f_ϕ values

If the ALP field starts oscillating at $T_{\rm osc}$, and the $n_\phi a^3 = \rho_\phi a^3/m_\phi$ is conserved afterwards:

$$h^2\Omega_{\phi,0} \approx 0.12\sqrt{\frac{m_0}{\rm eV}}\sqrt{\frac{m_0}{m_{\rm osc}}}\underbrace{\left(\frac{m_{\rm osc}}{3H_{\rm osc}}\right)^{3/2}}_{\sim\mathcal{O}(1)}\underbrace{\theta_i^2}_{<\pi^2}\left(\frac{f_\phi}{10^{11}\,\rm GeV}\right)^2\underbrace{\mathcal{F}(T_{\rm osc})}_{0.3\div1.0}.$$

- Modify the high temperature behavior of the ALP mass — Arias+ 1201.5902

$$m_\phi(T) \approx m_0 \times \begin{cases} (T_c/T)^\beta, & T > T_c \\ 1, & T < T_c \end{cases} \xrightarrow{T_c\sim\sqrt{m_0 f_\phi}} \sqrt{\frac{m_0}{m_{\rm osc}}} \sim \left(\frac{H_{\rm osc}}{m_{\rm osc}}\right)^{\frac{\beta/2}{\beta+2}}\left(\frac{M_{\rm pl}}{f_\phi}\right)^{\frac{\beta/2}{\beta+2}}$$

- Modify the initial conditions $\Longrightarrow$ Increase $m_{\rm osc}/3H_{\rm osc}$
  - **Large misalignment**: Tune the initial angle, $|\pi - \theta_i| \ll 1$ — Zhang,Chiueh 1705.01439; Arvanitaki+ 1909.11665
  - **Kinetic misalignment:** Start with a large initial kinetic energy. — Co et al. 1910.14152; Chang et al. 1911.11885
- Modify the potential to a non-periodic one $\Longrightarrow$ No bound on θ_i^2

$$V(\theta) = \frac{m_\phi^2 f_\phi^2}{2p}\left[\left(1+\theta^2\right)^p - 1\right], \quad p < 1$$

Ollé+. 1906.06352; Chatrchyan, **CE**, Koschnitzke, Servant 2305.03756

Extending the parameter space to lower f_ϕ values

If the ALP field starts oscillating at $T_{\rm osc}$, and the $n_\phi a^3 = \rho_\phi a^3/m_\phi$ is conserved afterwards:

$$h^2\Omega_{\phi,0} \approx 0.12\sqrt{\frac{m_0}{\rm eV}}\sqrt{\frac{m_0}{m_{\rm osc}}}\underbrace{\left(\frac{m_{\rm osc}}{3H_{\rm osc}}\right)^{3/2}}_{\sim\mathcal{O}(1)}\underbrace{\theta_i^2}_{<\pi^2}\left(\frac{f_\phi}{10^{11}\,\text{GeV}}\right)^2\underbrace{\mathcal{F}(T_{\rm osc})}_{0.3\div1.0}.$$

- Modify the high temperature behavior of the ALP mass — Arias+ 1201.5902

$$m_\phi(T) \approx m_0 \times \begin{cases} (T_c/T)^\beta, & T > T_c \\ 1, & T < T_c \end{cases} \quad \xrightarrow{T_c\sim\sqrt{m_0 f_\phi}} \quad \sqrt{\frac{m_0}{m_{\rm osc}}} \sim \left(\frac{H_{\rm osc}}{m_{\rm osc}}\right)^{\frac{\beta/2}{\beta+2}}\left(\frac{M_{\rm pl}}{f_\phi}\right)^{\frac{\beta/2}{\beta+2}}$$

- Modify the initial conditions $\Longrightarrow$ Increase $m_{\rm osc}/3H_{\rm osc}$
  - **Large misalignment**: Tune the initial angle, $|\pi - \theta_i| \ll 1$ — Zhang,Chiueh 1705.01439; Arvanitaki+ 1909.11665
  - **Kinetic misalignment:** Start with a large initial kinetic energy. — Co et al. 1910.14152; Chang et al. 1911.11885
- Modify the potential to a non-periodic one $\Longrightarrow$ No bound on θ_i^2

$$V(\theta) = \frac{m_\phi^2 f_\phi^2}{2p}\left[\left(1+\theta^2\right)^p - 1\right], \quad p < 1$$

— Ollé+. 1906.06352; Chatrchyan, **CE**, Koschnitzke, Servant 2305.03756

Extending the parameter space to lower f_ϕ values

If the ALP field starts oscillating at $T_{\rm osc}$, and the $n_\phi a^3 = \rho_\phi a^3/m_\phi$ is conserved afterwards:

$$h^2\Omega_{\phi,0} \approx 0.12\sqrt{\frac{m_0}{\rm eV}}\sqrt{\frac{m_0}{m_{\rm osc}}}\underbrace{\left(\frac{m_{\rm osc}}{3H_{\rm osc}}\right)^{3/2}}_{\sim\mathcal{O}(1)}\underbrace{\theta_i^2}_{<\pi^2}\left(\frac{f_\phi}{10^{11}\,\text{GeV}}\right)^2\underbrace{\mathcal{F}(T_{\rm osc})}_{0.3\div1.0}.$$

- Modify the high temperature behavior of the ALP mass — Arias+ 1201.5902

$$m_\phi(T) \approx m_0 \times \begin{cases}(T_c/T)^\beta, & T > T_c\\ 1, & T < T_c\end{cases} \quad \xrightarrow{T_c\sim\sqrt{m_0 f_\phi}} \quad \sqrt{\frac{m_0}{m_{\rm osc}}} \sim \left(\frac{H_{\rm osc}}{m_{\rm osc}}\right)^{\frac{\beta/2}{\beta+2}}\left(\frac{M_{\rm pl}}{f_\phi}\right)^{\frac{\beta/2}{\beta+2}}$$

- Modify the initial conditions $\Longrightarrow$ Increase $m_{\rm osc}/3H_{\rm osc}$
  - **Large misalignment**: Tune the initial angle, $|\pi - \theta_i| \ll 1$ — Zhang,Chiueh 1705.01439; Arvanitaki+ 1909.11665
  - **Kinetic misalignment:** Start with a large initial kinetic energy. — Co et al. 1910.14152; Chang et al. 1911.11885
- Modify the potential to a non-periodic one $\Longrightarrow$ No bound on θ_i^2

$$V(\theta) = \frac{m_\phi^2 f_\phi^2}{2p}\left[\left(1+\theta^2\right)^p - 1\right], \quad p < 1$$

Ollé+. 1906.06352; Chatrchyan, **CE**, Koschnitzke, Servant 2305.03756

Extending the parameter space to lower f_ϕ values

If the ALP field starts oscillating at $T_{\rm osc}$, and the $n_\phi a^3 = \rho_\phi a^3/m_\phi$ is conserved afterwards:

$$h^2\Omega_{\phi,0} \approx 0.12\sqrt{\frac{m_0}{\rm eV}}\sqrt{\frac{m_0}{m_{\rm osc}}}\underbrace{\left(\frac{m_{\rm osc}}{3H_{\rm osc}}\right)^{3/2}}_{\sim\mathcal{O}(1)}\underbrace{\theta_i^2}_{<\pi^2}\left(\frac{f_\phi}{10^{11}\,\text{GeV}}\right)^2\underbrace{\mathcal{F}(T_{\rm osc})}_{0.3\div1.0}.$$

- Modify the high temperature behavior of the ALP mass — Arias+ 1201.5902

$$m_\phi(T) \approx m_0 \times \begin{cases} (T_c/T)^\beta, & T > T_c \\ 1, & T < T_c \end{cases} \quad \xrightarrow{T_c\sim\sqrt{m_0 f_\phi}} \quad \sqrt{\frac{m_0}{m_{\rm osc}}} \sim \left(\frac{H_{\rm osc}}{m_{\rm osc}}\right)^{\frac{\beta/2}{\beta+2}}\left(\frac{M_{\rm pl}}{f_\phi}\right)^{\frac{\beta/2}{\beta+2}}$$

- Modify the initial conditions $\Longrightarrow$ Increase $m_{\rm osc}/3H_{\rm osc}$
  - **Large misalignment**: Tune the initial angle, $|\pi - \theta_i| \ll 1$ — Zhang,Chiueh 1705.01439; Arvanitaki+ 1909.11665
  - **Kinetic misalignment:** Start with a large initial kinetic energy. — Co et al. 1910.14152; Chang et al. 1911.11885
- Modify the potential to a non-periodic one $\Longrightarrow$ No bound on θ_i^2

$$V(\theta) = \frac{m_\phi^2 f_\phi^2}{2p}\left[\left(1+\theta^2\right)^p - 1\right], \quad p < 1$$

Ollé+. 1906.06352; Chatrchyan, **CE**, Koschnitzke, Servant 2305.03756

The Large Misalignment mechanism

If the initial angle is very close to $\pm\pi$, the onset of oscillations got delayed due to the tiny potential gradient at the top: Arvanitaki et al. 1909.11665

$$\frac{t_{\rm osc}^{\rm LMM}}{t_{\rm osc}^{\rm SMM}} \sim \ln\left[\frac{1}{\pi - |\theta_i|}\frac{2^{1/4}\pi^{1/2}}{\Gamma(5/4)}\right]$$

This enhances the relic density, albeit logarithmically. Therefore, large tunings† are required for significant enhancements.

† : Can also be natural in some models. Co et al. 1812.11192

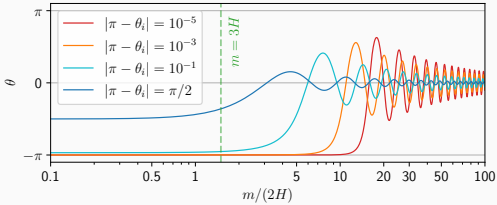

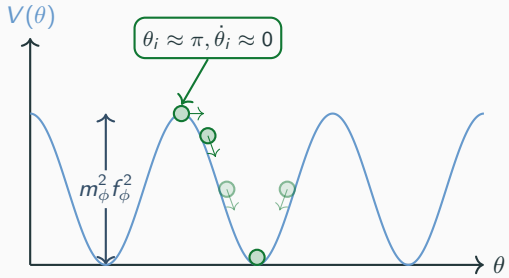

The Kinetic Misaligment Mechanism

A large initial kinetic energy for the ALP field can be motivated in various UV completions:

- Explicit breaking of the PQ symmetry in deep UV.
  Co et al. 1910.14152; 2004.00629; 2006.05687
  CE, Servant, Sørensen, Sato 2408.08355
- Trapped misalignment Luzio et al. 2102.00012; 2102.01082

Today's ALP energy density is Co et al. 1910.14152
CE, Servant, Sørensen, Sato 2206.14259

$$h^2\Omega_{\phi,0} \approx 0.12\left(\frac{m_\phi}{5\times10^{-3}\,\mathrm{eV}}\right)\left(\frac{Y}{40}\right), \qquad Y = \frac{f_\phi \dot{\phi}(T)}{s(T)}$$

The yield parameter Y is conserved after the kick, and determines the ALP relic density today.

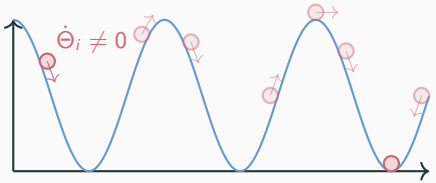

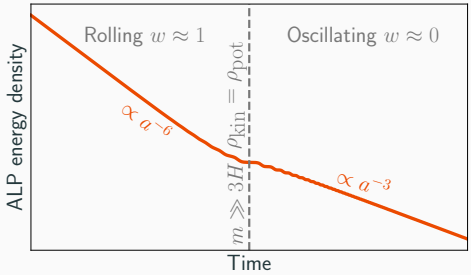

ALP dark matter parameter space (with KSVZ-like photon coupling $g_{\theta\gamma} = (\alpha_{\rm em}/2\pi)(1.92/f_\phi)$)

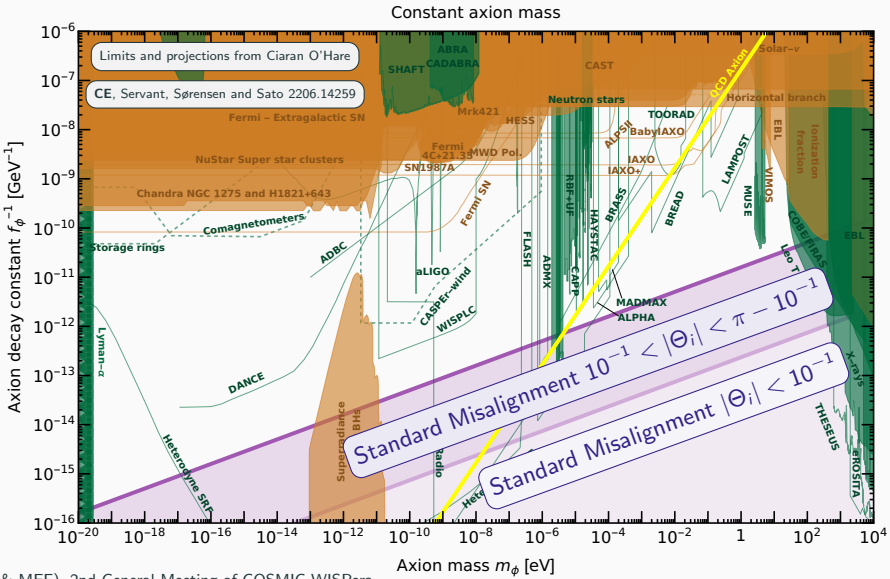

ALP dark matter parameter space (with KSVZ-like photon coupling $g_{\theta\gamma} = (\alpha_{\rm em}/2\pi)(1.92/f_\phi)$)

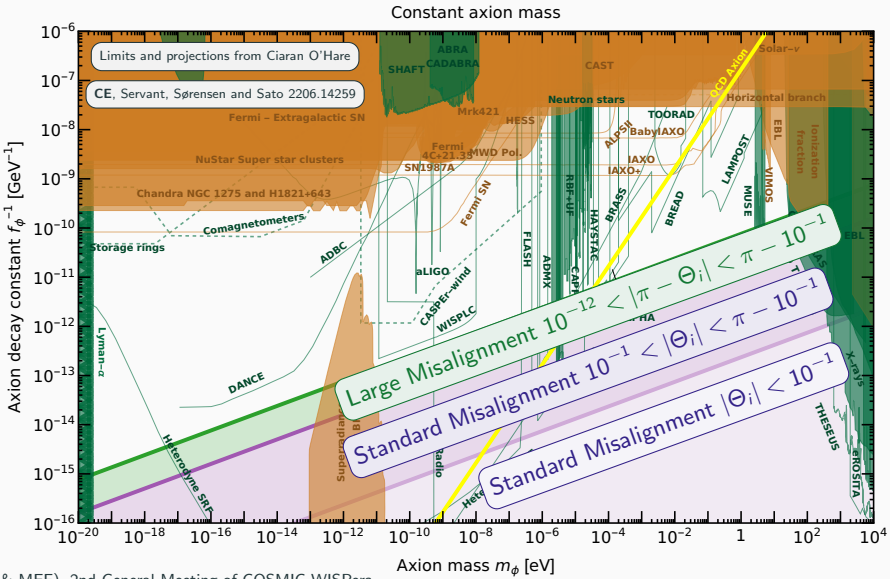

ALP dark matter parameter space (with KSVZ-like photon coupling $g_{\theta\gamma} = (\alpha_{\mathbf{em}}/2\pi)(1.92/f_\phi)$)

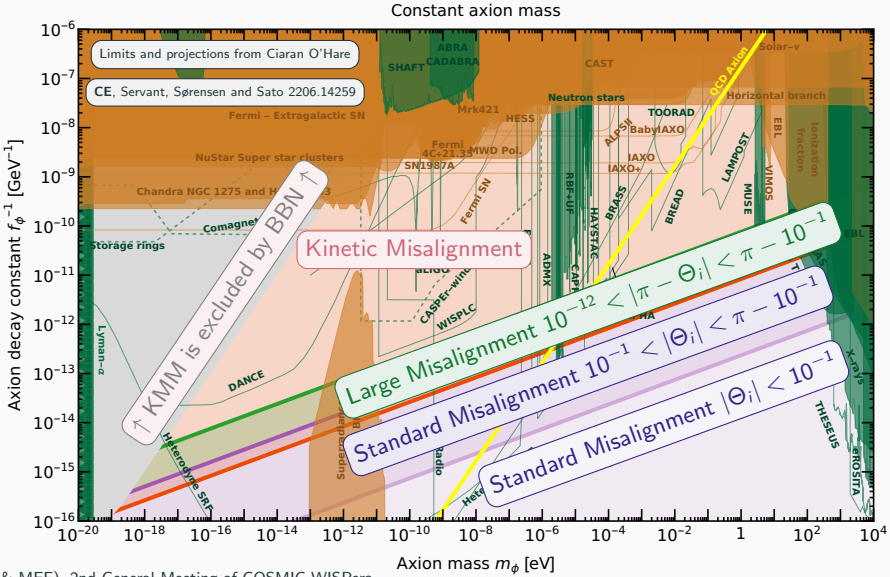

ALP dark matter parameter space (with KSVZ-like photon coupling $g_{\theta\gamma} = (\alpha_{\mathbf{em}}/2\pi)(1.92/f_\phi)$)

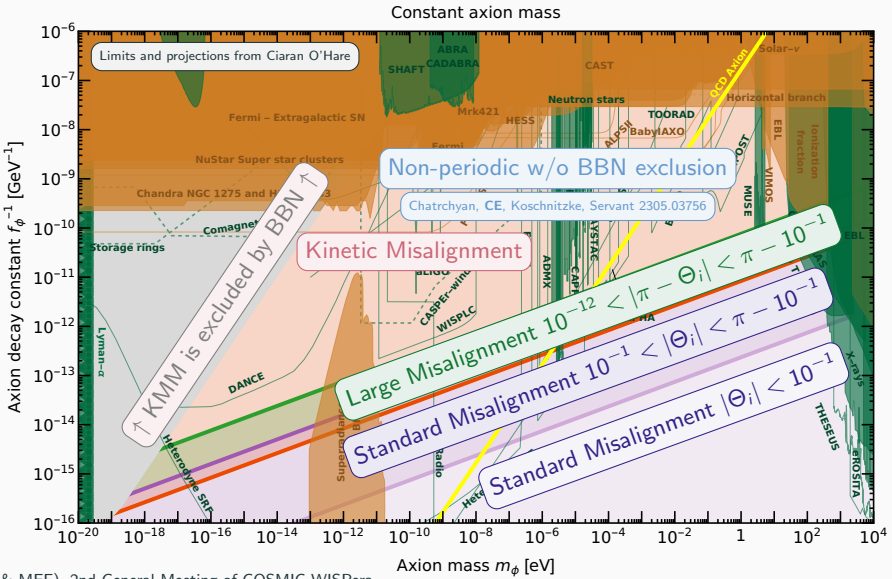

ALP dark matter parameter space in a specific Kinetic misalignment UV completion

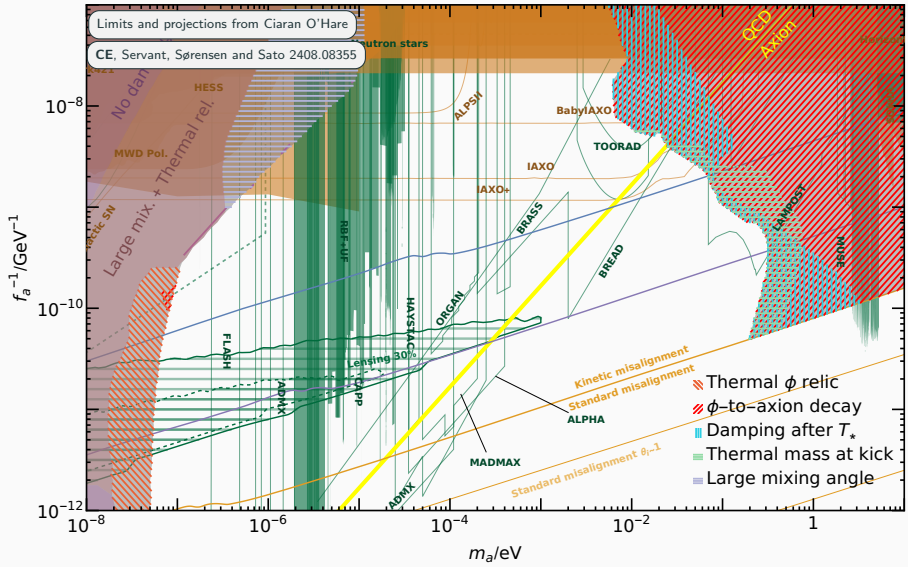

ALP fluctuations and the mode functions

- Even in the pre-inflationary scenario ALP field has some fluctuations on top of the homogeneous background which can be described by the mode functions in the Fourier space.

$$\theta(t, \mathbf{x}) = \Theta(t) + \int \frac{\mathrm{d}^3 k}{(2\pi)^3} \theta_k e^{i\vec{\mathbf{k}}\cdot\vec{\mathbf{x}}} + \text{h.c.}$$

- These fluctuations are seeded by adiabatic and/or isocurvature perturbations:

Adiabatic perturbations (This work)

- Due to the energy density perturbations of the dominating component, **unavoidable**.
- Initial conditions in the super-horizon limit:

$$\delta_i/(1 + w_i) = \delta_j/(1 + w_j)$$

Isocurvature perturbations

- If ALPs exist during inflation and are light $m \ll H_{\text{inf}}$, they pick up quantum fluctuations:

$$\delta\theta \sim H_{\text{inf}}/(2\pi f_{\text{inf}})$$

- Can be avoided/suppressed if ALP has a large mass during inflation, or $f_{\text{inf}} \gg f_{\text{today}}$.

Exponential growth of the mode functions

The equation of motion for the mode functions can be derived from the FRLW metric including the curvature perturbations:

$$\mathrm{d}s^2 = -[1-2\Phi(t,\mathbf{x})]+a^2(t)[1+2\Phi(t,\mathbf{x})]\delta_{ij}\,\mathrm{d}x^i\,\mathrm{d}x^j\,, \quad \Phi_k(t,\mathbf{x}) = 3\Phi_k(0)\left[\frac{\sin t_k - t_k\cos t_k}{t_k^3}\right],\ t_k = \frac{k/a}{\sqrt{3}H}$$

For small fluctuations $\delta\theta \ll \Theta$ the equation of motion for the mode functions become

$$\ddot{\phi}_k + 3H\dot{\phi}_k + \underbrace{\left[\frac{k^2}{a^2} + V''(\phi)\Big|_{\bar{\phi}}\right]}_{\text{eff. frequency}}\phi_k = \underbrace{2\,\Phi_k\ V'(\phi)\Big|_{\bar{\phi}} - 4\dot{\Phi}_k\dot{\bar{\phi}}}_{\text{source term}}$$

The EoM is unstable when the effective frequency

- becomes negative $\Rightarrow$ tachyonic instability
- is oscillating $\Rightarrow$ parametric resonance

Kofman et al. hep-ph/9704452; Felder, Kofman hep-ph/0606256

Greene et al. hep-ph/9808477; Jaeckel et al. 1605.01367

Cedeno et al. 1703.10180; Berges et al. 1903.03116

Fonseca et al. 1911.08472; Morgante et al. 2109.13823

Instability exists except for a free theory where $V''(\phi) = m^2$.

Exponential growth of the mode functions

The equation of motion for the mode functions can be derived from the FRLW metric including the curvature perturbations:

$$\mathrm{d}s^2 = -[1-2\Phi(t,\mathbf{x})]+a^2(t)[1+2\Phi(t,\mathbf{x})]\delta_{ij}\,\mathrm{d}x^i\,\mathrm{d}x^j\,, \quad \Phi_k(t,\mathbf{x}) = 3\Phi_k(0)\left[\frac{\sin t_k - t_k\cos t_k}{t_k^3}\right],\ t_k = \frac{k/a}{\sqrt{3}H}$$

For small fluctuations $\delta\theta \ll \Theta$ the equation of motion for the mode functions become

$$\ddot{\phi}_k + 3H\dot{\phi}_k + \underbrace{\left[\frac{k^2}{a^2} + V''(\phi)\Big|_{\bar{\phi}}\right]}_{\text{eff. frequency}}\phi_k = \underbrace{2\,\Phi_k\ V'(\phi)\Big|_{\bar{\phi}} - 4\dot{\Phi}_k\dot{\bar{\phi}}}_{\text{source term}}$$

The EoM is unstable when the effective frequency

- becomes negative $\Rightarrow$ tachyonic instability
- is oscillating $\Rightarrow$ parametric resonance

Kofman et al. hep-ph/9704452; Felder, Kofman hep-ph/0606256

Greene et al. hep-ph/9808477; Jaeckel et al. 1605.01367

Cedeno et al. 1703.10180; Berges et al. 1903.03116

Fonseca et al. 1911.08472; Morgante et al. 2109.13823

Instability exists except for a free theory where $V''(\phi) = m^2$.

Exponential growth of the mode functions

The equation of motion for the mode functions can be derived from the FRLW metric including the curvature perturbations:

$$\mathrm{d}s^2 = -[1-2\Phi(t,\mathbf{x})]+a^2(t)[1+2\Phi(t,\mathbf{x})]\delta_{ij}\,\mathrm{d}x^i\,\mathrm{d}x^j\,, \quad \Phi_k(t,\mathbf{x}) = 3\Phi_k(0)\left[\frac{\sin t_k - t_k\cos t_k}{t_k^3}\right],\ t_k = \frac{k/a}{\sqrt{3}H}$$

For small fluctuations $\delta\theta \ll \Theta$ the equation of motion for the mode functions become

$$\ddot{\phi}_k + 3H\dot{\phi}_k + \underbrace{\left[\frac{k^2}{a^2} + V''(\phi)\Big|_{\bar{\phi}}\right]}_{\text{eff. frequency}}\phi_k = \underbrace{2\,\Phi_k\ V'(\phi)\Big|_{\bar{\phi}} - 4\dot{\Phi}_k\dot{\bar{\phi}}}_{\text{source term}}$$

The EoM is unstable when the effective frequency

- becomes negative $\Rightarrow$ tachyonic instability
- is oscillating $\Rightarrow$ parametric resonance

Kofman et al. hep-ph/9704452; Felder, Kofman hep-ph/0606256

Greene et al. hep-ph/9808477; Jaeckel et al. 1605.01367

Cedeno et al. 1703.10180; Berges et al. 1903.03116

Fonseca et al. 1911.08472; Morgante et al. 2109.13823

Instability exists except for a free theory where $V''(\phi) = m^2$.

After the parametric resonance the power spectrum can reach to $\mathcal{O}(1)$ values

Dense and compact ALP mini-clusters can also be formed in the pre-inflationary scenario!

Growth rate of the perturbations depend exponentially on $m_\phi/H\big|_{\rm osc}$.

$$\text{Smaller } f_\phi \implies \text{Larger } \frac{m_{\rm osc}}{H_{\rm osc}}$$

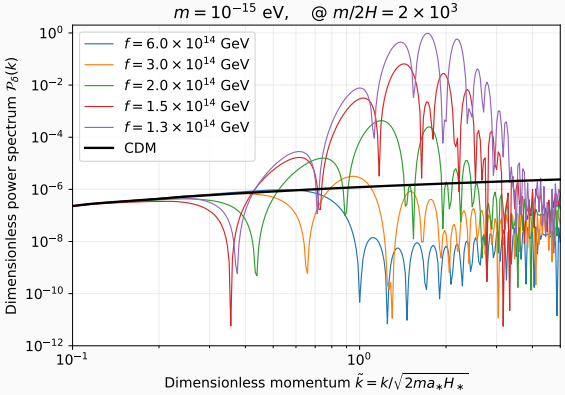

Breakdown of linearity and complete fragmentation

When the power spectrum becomes $\mathcal{O}(1)$, the linear perturbation theory breaks down, and the ALP field becomes completely fragmented. This regime can be studied by

- Semi-analytically via an energy conservation argument. Used for the Kinetic misalignment.
  Fonseca et al. 1911.08472; **CE**, Servant, Sørensen, Sato 2206.14259
- Fully numerically using lattice simulations. Used for the non-periodic potentials.
  Morgante et al. 2109.13823; Chatrchyan, **CE**, Koschnitzke, Servant 2305.03756

The non-linear effects smoothens out the power spectrum, so in the non-linear regime more efficient parametric resonance yields a power spectrum with smaller peaks.

For a given ALP mass m_ϕ and a production mechanism such as SMM, KMM, non-periodic etc..., there is a critical f_ϕ that yields the most peaked power spectrum, hence most dense structures.

Breakdown of linearity and complete fragmentation

When the power spectrum becomes $\mathcal{O}(1)$, the linear perturbation theory breaks down, and the ALP field becomes completely fragmented. This regime can be studied by

- Semi-analytically via an energy conservation argument. Used for the Kinetic misalignment.
  Fonseca et al. 1911.08472; **CE**, Servant, Sørensen, Sato 2206.14259
- Fully numerically using lattice simulations. Used for the non-periodic potentials.
  Morgante et al. 2109.13823; Chatrchyan, **CE**, Koschnitzke, Servant 2305.03756

The non-linear effects smoothens out the power spectrum, so in the non-linear regime more efficient parametric resonance yields a power spectrum with smaller peaks.

For a given ALP mass m_ϕ and a production mechanism such as SMM, KMM, non-periodic etc..., there is a critical f_ϕ that yields the most peaked power spectrum, hence most dense structures.

Breakdown of linearity and complete fragmentation

When the power spectrum becomes $\mathcal{O}(1)$, the linear perturbation theory breaks down, and the ALP field becomes completely fragmented. This regime can be studied by

- Semi-analytically via an energy conservation argument. Used for the Kinetic misalignment.
  Fonseca et al. 1911.08472; **CE**, Servant, Sørensen, Sato 2206.14259
- Fully numerically using lattice simulations. Used for the non-periodic potentials.
  Morgante et al. 2109.13823; Chatrchyan, **CE**, Koschnitzke, Servant 2305.03756

The non-linear effects smoothens out the power spectrum, so in the non-linear regime more efficient parametric resonance yields a power spectrum with smaller peaks.

For a given ALP mass m_ϕ and a production mechanism such as SMM, KMM, non-periodic etc..., there is a critical f_ϕ that yields the most peaked power spectrum, hence most dense structures.

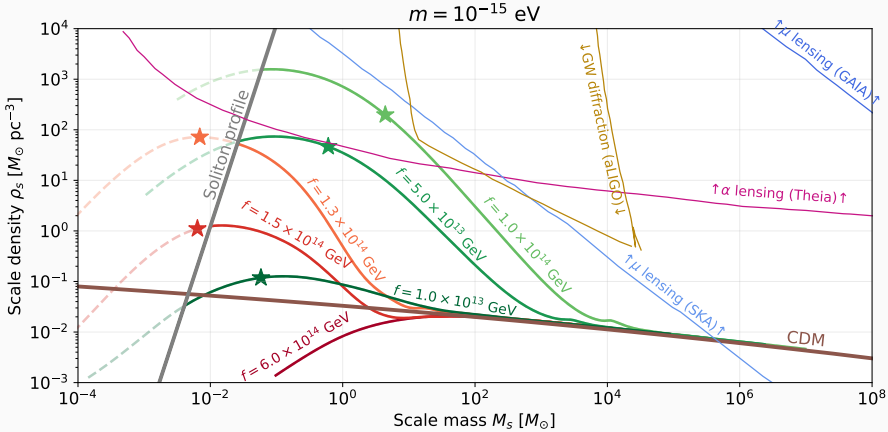

Calculated semi-analytically using the Excursion Set Formalism assuming NFW profile, but setting the soliton line as a cutoff. Stars denote the local maxima of the Halo mass function.

Observational prospects

Chatrchyan, CE, Koschnitzke, Servant 2305.03756

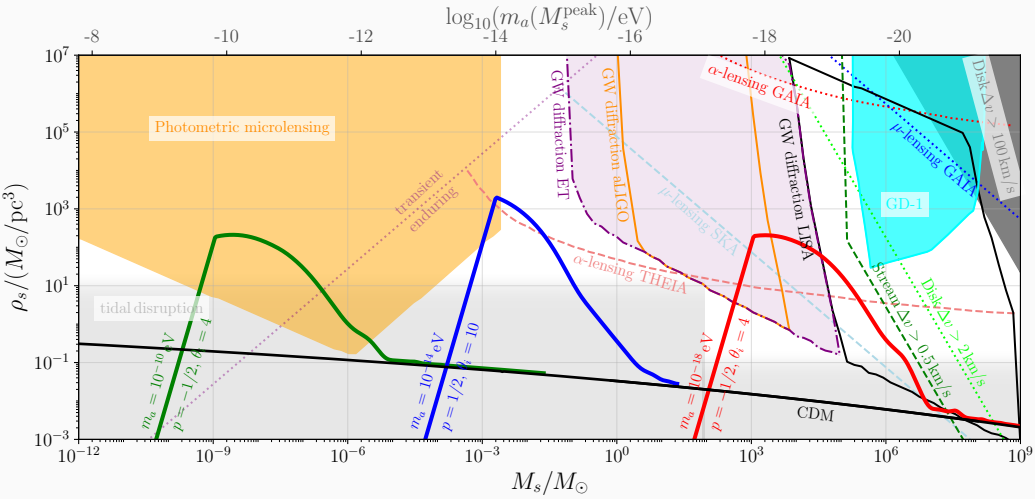

Experimental prospects from Tilburg et al. 1804.01991; Arvanitaki et al. 1909.11665; Ramani et al. 2005.03030

Dense halo region in the ALP parameter space

Chatrchyan, CE, Koschnitzke, Servant 2305.03756

Shaded regions indicate the parameter space where parametric resonance might create halos with $\rho_s \gtrsim 10\, M_\odot\, \mathrm{pc}^{-3}$ which are more likely to survive tidal stripping Arvanitaki et al. 1909.11665.

The "dense halo regions" in different production mechanisms mostly overlap with each other. So, it is difficult to infer the mechanism from observations.

However, observation of dense structures gives us information about the ALP mass and the decay constant even when ALP does not couple to SM!

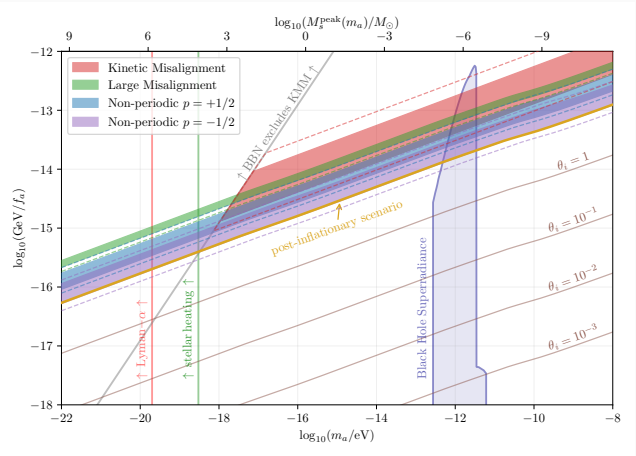

Dense halo region in the ALP parameter space

Chatrchyan, CE, Koschnitzke, Servant 2305.03756

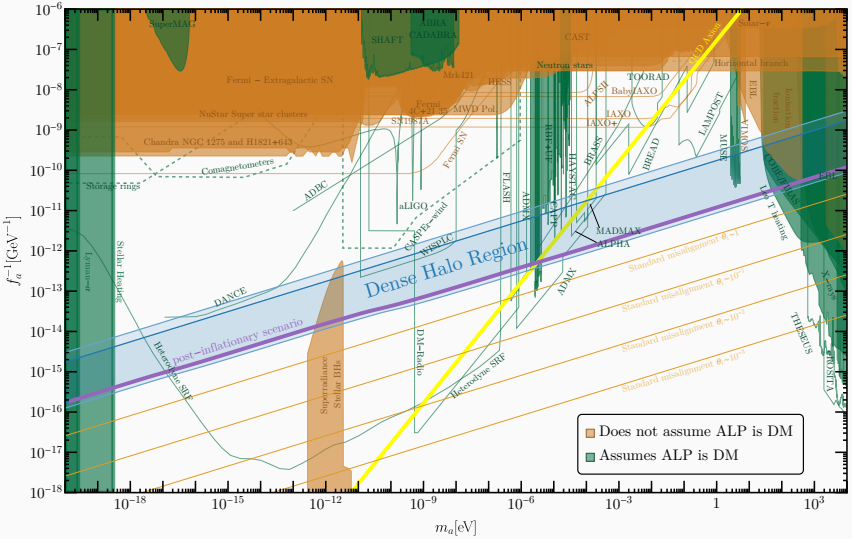

Open questions

- How does the ALP relic density is affected by complete fragmentation?
- Implications of complete fragmentation on ALP experiments, such as haloscopes. O'Hare+ 2311.17367
- Effect of the parametric resonance on the Lyman alpha bounds. Winch+ 2311.02052
- Mini-clusters in the post-inflationary scenario vs mini-clusters via parametric resonance

Conclusions and Outlook

- The Standard Misalignment Mechanism is not sufficient to account for the correct dark matter abundance in the ALP parameter space where the experiments are most sensitive.
- This parameter space can be opened by considering models where the initial energy budget is increased, and the onset of oscillations is delayed from the conventional value $m_{\rm osc}/H_{\rm osc} \sim 3$.
- In these models which go beyond the standard paradigm, the fluctuations can grow exponentially, and dense ALP mini-clusters can be formed even in the pre-inflationary scenario.
- Our semi-analytical study predicts that there is a band on the (m_ϕ, f_ϕ)-plane where the dense structures can be formed, and the location of this band does not depend drastically on the production mechanism.
- The existence of this band allows us to obtain information about the decay constant, even if ALP does not couple to the Standard Model.

Thank you for listening!

Cem Eröncel
0000-0002-9308-1449
cem.eroncel@itu.edu.tr

Cosmological evolution of the ALP field

Start with the action for the ALP field (neglect Standard Model interactions):

$$S = \int \mathrm{d}^4x \sqrt{-g}[-g^{\mu\nu}\partial_\mu\phi\partial_\nu\phi - V(\phi)].$$

Take the background geometry to be the FRWL geometry with the metric

$$\mathrm{d}s^2 = -\mathrm{d}t^2 + a^2(t)\delta_{ij}\,\mathrm{d}x^i\,\mathrm{d}x^j$$

Then, the ALP field obeys the following equation of motion:

$$\ddot{\theta} + 3H\dot{\theta} - \frac{\nabla^2}{a^2}\theta + \frac{1}{f_\phi^2}\frac{\mathrm{d}V}{\mathrm{d}\theta} = 0, \quad H = \frac{\dot{a}}{a} := \text{Hubble parameter.}$$

This is a second order ODE which can be solved after specifying the initial conditions.

Evolution of the density contrast at late times

Calculating the evolution of the density contrast until today by numerically solving the mode function equation of motion is very time- and resource-consuming. Luckily, we can use an effective description using the WKB approximation: Park et al., 1207.3124

$$\Theta(t) = a^{-3/2}[\Theta_+ \cos(mt) + \Theta_- \sin(mt)],$$
$$\theta_k(t) = \theta_+(k,t)\cos(mt) + \theta_-(k,t)\sin(mt).$$

The evolution of the density contrast for sub-horizon modes, $k/a \gg H$ obeys the differential equation (valid both in radiation and matter eras):

$$\ddot{\delta}_k + 2H\dot{\delta}_k + \left(c_{s,\mathrm{eff}}^2 \frac{k^2}{a^2} - 4\pi G\overline{\rho}\right)\delta_k = 0, \quad \overbrace{c_{s,\mathrm{eff}}^2 \approx \frac{1}{4}\frac{k^2}{a^2 m^2}\left(1 + \frac{1}{4}\frac{k^2}{a^2 m^2}\right)^{-1} \approx \frac{1}{4}\frac{k^2}{a^2 m^2}}^{\text{effective sound speed of the ALP}}.$$

The evolution for Cold Dark Matter (CDM) is recovered in the limit $c_{s,\mathrm{eff}}^2 \to 0$ or $m \to \infty$.

Axion Jeans Scale

For sub-horizon $k/a \gg H$ and non-relativistic $k/a \ll m$ modes, the density contrast evolution is

$$\ddot{\delta}_k + 2H\dot{\delta}_k + \left[\underbrace{\frac{1}{4}\frac{(k/a)^4}{m^2}}_{\text{"pressure" term}} - \underbrace{4\pi G\overline{\rho}}_{\substack{\text{gravitational} \\ \text{instability}}} \right] \delta_k = 0.$$

The scale at which the "pressure" term and gravitational instability becomes equal is called the Axion Jeans scale:

$$k_J(a) = (16\pi G a \overline{\rho})^{1/4}\sqrt{m} = 66.5 \times a^{1/4}\left(\frac{h^2\Omega_\Theta}{h^2\Omega_{\rm DM}}\right)\sqrt{\frac{m}{10^{-22}\,\mathrm{eV}}}\,\mathrm{Mpc}^{-1}.$$

The behavior of the density contrast depends whether it is above or below the Jeans scale:

- Modes above the Jeans scale oscillate with a frequency given by the effective sound speed both in matter- and radiation-domination.
- Modes below the Jeans scale behaves like CDM. They grow logarithmically during the radiation era, and linearly during the matter era.

Gravitational collapse

Once the matter fluctuations become sufficiently dense, they decouple from the ambient Hubble flow, and form gravitationally bound structures known as halos. This process is called gravitational collapse. Studying this process precisely is quite difficult, and requires N-body simulations. However, qualitative results can be derived by exploiting the approximate spherical symmetry.

Consider a spherical overdensity δ with physical radius r:

$$M = \frac{4\pi}{3}\bar{\rho}(1+\delta)r^3$$

Assume that the mass M in the overdense region is constant during the collapse. The evolution of the physical radius r obeys the differential equation:

$$\ddot{r} = -\underbrace{\frac{MG}{r^2}}_{\text{matter}} - \underbrace{\frac{8\pi G}{3}\rho_r r}_{\text{radiation}}$$

Critical density at collapse

During the evolution, the physical radius r first decouples from the Hubble flow, then turns around, and finally collapses. The redshifts at which these events occur depends on the size of the initial overdensity δ_i:

$$\left.\frac{a}{a_{\rm eq}}\right|_{\rm turnaround} \approx \frac{0.7}{\delta_i} \quad , \quad \left.\frac{a}{a_{\rm eq}}\right|_{\rm collapse} \approx \frac{1.1}{\delta_i}$$

Prediction of the linear theory at the time of collapse gives the critical density at collapse:

Ellis et al. 2006.08637; **CE** and Servant, 2207.10111

$$\delta_c(a_c) \approx \left(\frac{1.1}{a_c/a_{\rm eq}}\right)\left(1+\frac{3}{2}\frac{a_c}{a_{\rm eq}}\right).$$

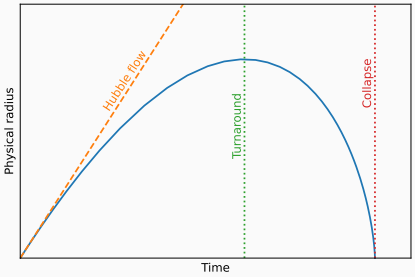

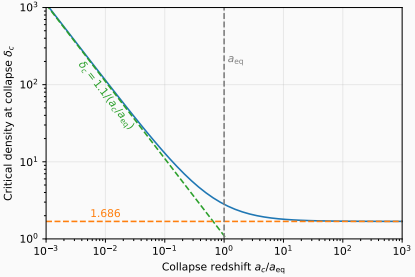

Press-Schechter Formalism

The formation of the dark matter halos can be studied analytically via the Press-Schechter (PS) formalism. Let us define the following quantities: Press and Schechter, '74

- $\mathscr{F}(>M;a)$: The fraction of matter which is inside collapsed structures of comoving size larger than R at any given scale factor a.
- $\mathscr{P}(\delta_R(a)>\delta_c(a))$: The probability of finding an overdensity $\delta_R(\mathbf{x},a)>\delta_c(a)$ where $\delta_R(\mathbf{x},a)$ is the overdensity *smoothed* at the scale R, and $\delta_c(a)$ is the critical density for collapse at scale factor a.

The PS postulate states that these quantities are equal:

$$\mathscr{F}(>M;a)=\mathscr{P}(\delta_R(a)>\delta_c(a))$$

The smoothe density contrast is obtained via a window function:

$$\delta_R(\mathbf{x},a)=\int \mathrm{d}^3\mathbf{x}'\, W_R(|\mathbf{x}-\mathbf{x}'|)\delta(\mathbf{x}',a), \qquad \int \mathrm{d}^3\mathbf{x}\, W_R(\mathbf{x})=1,$$

The variance of the smoothed density contrast is

$$\sigma_R^2(a)=\left\langle |\delta_R(\mathbf{x},a)|^2\right\rangle=\int_0^\infty \frac{\mathrm{d}k}{k}\left|\widetilde{W}_R(k)\right|^2\mathcal{P}_\delta(k;a),$$

Halo mass function (HMF)

An important observable of a dark matter model is the halo mass function (HMF) which gives the number density of halos per logarithmic mass bin:

$$\frac{\mathrm{d}n(M;a)}{\mathrm{d}\ln M} = \frac{1}{2}\frac{\overline{\rho}_{m,0}}{M} f_{\mathrm{PS}}\left(\frac{\delta_c(a)}{\sigma_M(a)}\right)\left|\frac{\mathrm{d}\ln\sigma_M^2(a)}{\mathrm{d}\ln M}\right|, \quad f_{\mathrm{PS}}(\nu) = \sqrt{\frac{2}{\pi}}\,\nu\exp\left(-\frac{\nu^2}{2}\right)$$

The relation between the mass of the halo M and the comoving radius R depends on the window function. For a spherical top-hat window function

$$W_{\mathrm{STH}}(\mathbf{x}) = \left(\frac{4\pi}{3}R^3\right)^{-1} \times \begin{cases} 1, & \mathbf{x} \leq R \\ 0, & \mathbf{x} > R \end{cases}.$$

The relation is

$$M(R) = \frac{4\pi}{3}\overline{\rho}a^3R^3 \approx \frac{4\pi}{3}\overline{\rho}_{m,0}a_0^3R^3,$$

This HMF is directly related to the luminosity function which quantifies the number of galaxies per luminosity interval.

Density profiles of dark matter halos

- Useful parameters to describe the dark matter halos:

$$\underbrace{\left.\frac{\partial \ln \rho(r)}{\partial \ln r}\right|_{r=r_s} = -2}_{\text{scale radius}}, \quad \underbrace{\rho_s = \rho(r = r_s)}_{\text{scale density}}, \quad \underbrace{M_s = \int_0^{r_s} \mathrm{d}^3\vec{\mathbf{r}}\, \rho(r) = 16\pi\rho_s r_s^3 \left(\ln 2 - \frac{1}{2}\right)}_{\text{scale mass}}.$$

- In order to determine these parameters, we need to know the density profile.

CDM

On all scales, the profile is well-approximated by the Navarro-Frenk-White (NFW) profile

Navarro et al. astro-ph/9611107

$$\rho_{\rm NFW}(r) = \frac{4\rho_s}{(r/r_s)(1 + r/r_s)^2}.$$

ALP

The profile is scale dependent:

- **Large scales:** NFW
- **Small scales:** Soliton Schive et al. 1406.6586

$$\rho_{\rm sol}(r) \approx \frac{2.9\rho_s}{\left(1 + \left(r/\sqrt{7}r_s\right)^2\right)^8} \Rightarrow \rho_s \propto m^6 M_s^4$$

- The scale density is closely related to the energy density at collapse:

$$\rho_s \propto \rho_c(z_{\rm col}) \Rightarrow \text{Fluctuations that collapse earlier create denser halos.}$$